

Development of the Wide Field Grism Spectrograph 2

Mariko Uehara^a, Chie Nagashima^a, Koji Sugitani^b, Makoto Watanabe^c, Shuji Sato^a, Tetsuya Nagata^a, Motohide Tamura^d, Noboru Ebizuka^e, Andrew J. Pickles^f, Klaus W. Hodapp^f, Yoichi Itoh^g, Makoto Nakano^h and Katsuo Oguraⁱ

^aDepartment of Physics, Nagoya University, Furo-cho, Chikusa-ku, Nagoya 464-8602, Japan;

^bInstitute of Natural Sciences, Nagoya City University, Mizuho-ku, Nagoya 467-8501, Japan;

^cSubaru Telescope, National Astronomical Observatory of Japan, Hilo, HI 96720, USA;

^dNational Astronomical Observatory of Japan, 2-21-1 Osawa, Mitaka, Tokyo 181-8588, Japan;

^eRIKEN, Wako, Saitama 351-0198, Japan;

^fInstitute for Astronomy, Hilo, HI 96720-270, USA;

^gGraduate School of Science and Technology, Kobe University, Nada-ku, Kobe 657-8501, Japan;

^hFaculty of Education and Welfare Science, Oita University, Oita 870-1192, Japan;

ⁱ4-10-28 Kokugakuin University, Higashi, Shibuya-ku, Tokyo 150-8440, Japan;

ABSTRACT

We have developed the Wide Field Grism Spectrograph 2 (WFGS2) for the f/10 focus of the University of Hawaii 2.2 m telescope (UH88). This instrument provides slit-less, wide-field spectroscopy as well as imaging and long-slit spectroscopy. Two CCD cameras of UH88, Tektronix 2k × 2k and OPTIC 4k × 4k, can be used as a detector. The spectral coverage is 380 - 970 nm, and the field of view is 11'.5 × 11'.5 with a pixel scale of 0".34 (Tektronix) or 0".21 pixel⁻¹ (OPTIC) in the imaging mode. WFGS2 has two replica gratings ($R = 620$ at 650 nm and $R = 730$ at 400 nm) and a Volume-Phase Holographic (VPH) grism ($R = 2500$ at 664 nm). The VPH grism enables intermediate-dispersion spectroscopy with this transmission system. Two long-slits with widths of 0".6 and 0".9 can be used. The Sloan Digital Sky Survey (g', r', i', z') and narrow-band (wide H α , H α , and [SII]+Li) filters are equipped. The first light observation was done in November 2003. We present the details of WFGS2, including the results of the first light observation.

Keywords: spectrograph, imager, optical

1. INTRODUCTION

Slit-less grism spectroscopy is a powerful tool for surveying emission line objects, such as H α emission line stars, Herbig-Haro objects, planetary nebulae, and so on. This was well demonstrated in a search of H α emission line stars and Herbig-Haro objects by Ogura, Sugitani and Pickles (2002)¹. They could detect candidates of weak-line T Tauri stars with H α equivalent widths of <1 Å down to $R = 20$ by using the Wide Field Grism Spectrograph (WFGS) at the UH88 telescope. A big advantage of slit-less grism spectroscopy over slit or multi-object fiber spectroscopy lies in its panoramic nature. It enables simultaneous multi-object spectroscopy inside the field of view (FOV) without pointing to each target. However, it is not easy to realize a wide FOV of a grism spectrograph so as to effectively survey large areas in the sky. For example, the FOV of WFGS is 5', not wide enough for wide area surveys, although it proves very deep survey capability due to the excellent seeing conditions of the Mauna Kea observing site. Thus it is worth constructing a new grism spectrograph with a wider FOV at the site of excellent seeing conditions. So we started to develop WFGS2 as a new grism spectrograph at the UH88 telescope.

Further author information: (Send correspondence to M.U.)

M.U.: E-mail: uehara@z.phys.nagoya-u.ac.jp, Telephone: +81-52-789-2925

WFGS2 is a compact, all transmission system which can be attached to the telescope beam in front of a CCD camera. It provides low and intermediate dispersion both in slit and slit-less spectroscopy. The FOV of 11'.5 is more than five times in area larger than that of WFGS. This instrument is rather optimized for slit-less spectroscopy, that is, we designed the optics so as to obtain good spectrum even at the corners of FOV. The spectroscopic resolution is optimized for the wavelengths around the H α and Ca HK lines although it becomes somewhat lower at the other wavelengths. Intermediate dispersion spectroscopy can be done with this transmission system by equipping a VPH grism. The characteristics of WFGS2 are summarized in Table 1 and the overall structure of WFGS2 is shown in Figure 1.

We present the optics and mechanics of WFGS2 in Sections 2 and 3 and the results of the first light observation in Section 4.

Table 1. Characteristics of WFGS2

Observation modes	imaging, slit-less spectroscopy, long-slit spectroscopy
Size	520 mm \times 640 mm \times 770 mm
Weight	50 kg (excluding CCD)
Optics	refractive optics
Wavelength coverage	380 - 970 nm
FOV	11'.5
Pixel scale	0".34 /pixel (Tektronix 2k)
f (collimator)	285 mm
f (camera)	185 mm
f-number	6.6
Detector	Tektronix2k \times 2kCCD, 24 μ m/pixel or OPTIC4k \times 4kCCD, 15 μ m/pixel

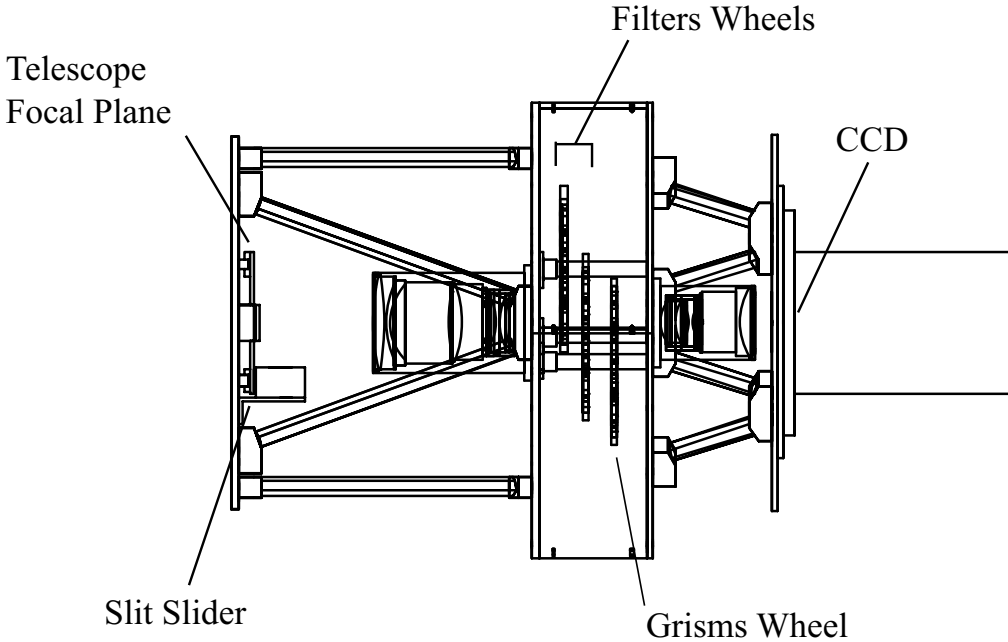


Figure 1. Overview of WFGS2. Left to the UH88 telescope.

2. OPTICS

2.1. Optics design

The optical layouts of WFGS2 are shown in Figure 2. The upper figure shows an imaging mode layout and the lower one shows a slit-less spectroscopic mode layout. The light from the UH88 telescope is collimated by the collimator and focused onto the CCD plane by the camera after passing through a filter and/or a grism. This optics system consists of 9 lenses. The collimator has 5 elements in 3 groups and the camera 4 elements in 2 groups. The collimator focal length is 285 mm and the camera focal length is 185 mm. Thus, the f-number of WFGS2 is 6.6, providing a magnification of 2/3. The length of the collimated beam, 188 mm, is long enough to insert a filter and/or a grism. The image size on the CCD does not change when the focus of WFGS2 moves because of telecentric lens system.

The spot diagrams of WFGS2 are shown in Figure 3. Figure 3a shows the spot diagrams of the imaging mode, Figures 3b and 3c are those in the spectroscopic mode for a replica grism of 300 gr/mm and for a VPH grism of 1315 gr/mm, at four CCD positions (1: center, 2: left, 3: top center, 4: upper left). A square shown on each spot diagram is 2 pixel \times 2 pixel ($48 \mu\text{m} \times 48 \mu\text{m}$) size of the Tektronix CCD camera. In the optics design, the 80 % encircled energy of spots is within $24 \mu\text{m}$ radius. The pixel scale of WFGS2 is $0''.34$ (Tektronix 2k). This is about half of typical seeing size atop Mauna Kea of $0''.6 - 0''.7$. The distortion of the imaging mode is below 0.1 %. The usable wavelength band is 380 - 970 nm, and the parfocal band when we adjust the focus at $\lambda = 550 \text{ nm}$ is 380 - 770 nm. If we adjust the focus at a certain wavelength, better spots can be obtained.

All of the lenses are treated with anti-reflection coating. The coat type is not multi-layer but single-layer coat so as to realize broad wavelength coverage. The transmission efficiencies of WFGS2 are 63 % at g' -band, 73 % at r' , 62 % at i' , 55 % at z' .

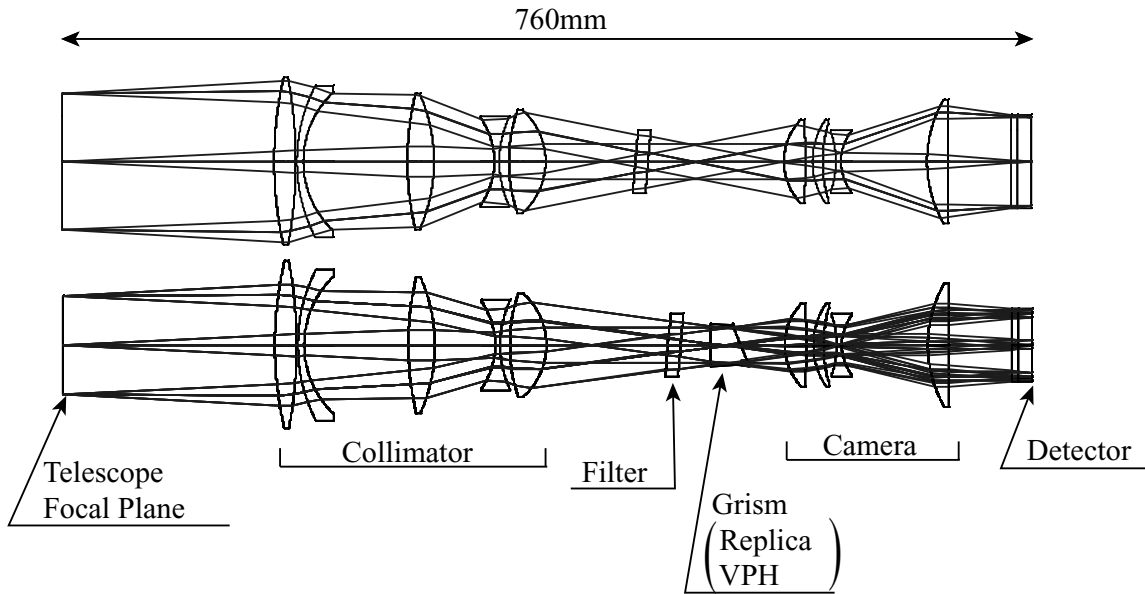


Figure 2. Optical layouts of WFGS2. The upper figure shows an imaging mode layout and the lower figure a slit-less spectroscopic mode layout.

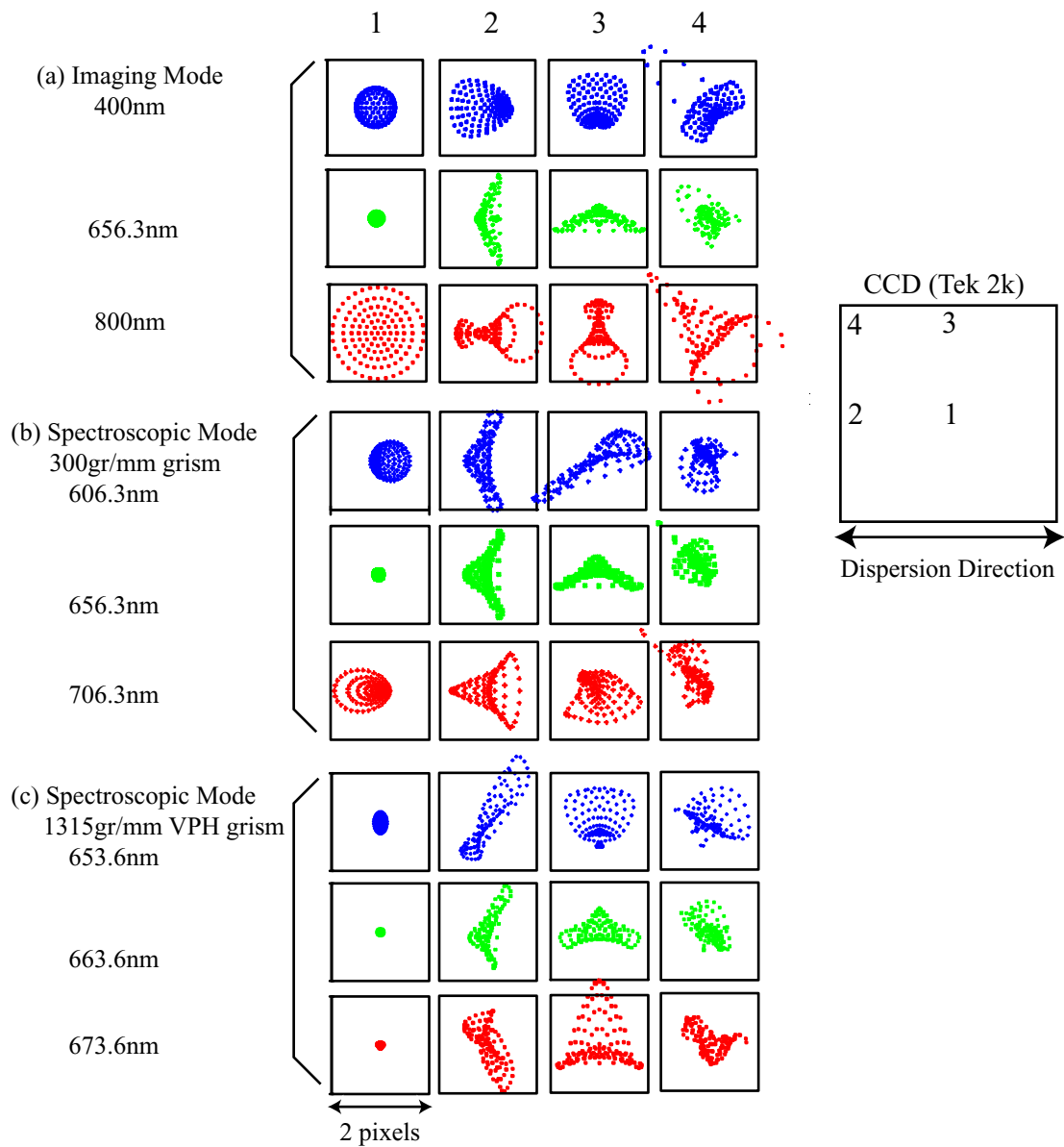


Figure 3. Spot diagrams of WFGS2 at four CCD positions (1: center, 2: left, 3: top center, 4: upper left). A square of each spot diagram is 2 pixel \times 2 pixel ($48 \mu\text{m} \times 48 \mu\text{m}$) with Tektronix CCD.

2.2. Slits

WFGS2 has two slits with widths of $65\ \mu\text{m}$ ($0''.6$) and $100\ \mu\text{m}$ ($0''.9$). The length of each slit, $75\ \text{mm}$ ($11'.5$), is very long. We can choose one of them depending on the seeing conditions.

2.3. Filters

WFGS2 provides 4 broad-band and 3 narrow-band filters at present. The broad-band filters are SDSS (g' , r' , i' , z') filters². The lists of filters are shown in Table 2. Filters of $50\ \text{mm}$ or $50.8\ \text{mm}$ (2 inch) square with thickness of $\leq 10\ \text{mm}$ can be attached with 5° tilted filter holders.

Table 2. Filters

	Filters	Effective wavelength (nm)	Bandwidth (nm)
Broad-band (SDSS)	g'	482.5	50
	r'	626.1	50
	i'	767.2	50
	z'	909.7	60
Narrow-band	wide H α	651.5	25
	H α	656.3	10
	[SII]+Li	672.0	10

2.4. Grisms

WFGS2 is equipped with three grisms. Two of them are replica grisms, and one VPH grism^{3,4}. The design specifications of each grism are shown in Table 3. The measured performance in the first light observation is indicated in Section 4.3.

Here we refer to conventional surface-relief grisms as replica grisms in order to distinguish them from VPH grisms, which have been developed recently. For intermediate dispersion, these grisms have higher diffraction efficiency than replica grisms since they do not have diffraction anomaly. The VPH grism has two prisms and a VPH grating which is sandwiched between prisms.

Table 3. Grisms (design values)

Grisms	R	λ_u (nm)	gr/mm	α (deg)
Replica grism 1	620	650	300	22.25
Replica grism 2	730	346	600	22.6
VPH grism	2500	664	1315	16×2

R : resolution ($\lambda/\Delta\lambda$) for $0''.9$ slit width,

λ_u : undeviated wavelength,

α : apex angle of the prism

3. MECHANICS

The outside picture of WFGS2 and the inside one of the wheel box are shown in Figure 4. The cross sectional view is presented in Figure 1. WFGS2 has a truss structure with a wheel box. This truss structure enables us to reduce the total weight of WFGS2 to 50kg without CCD. The slit slider is located at the focal plane of the UH88 telescope. The shutter is located just before the detector. Three wheels are contained inside the wheel box. The upper one is for grisms and lower two wheels are for filters. Each filter wheel can be equipped with up to 5 filters and the grism wheel 3 grisms. The slit slider and filter/grism wheels are driven by 4 stepping motors. These motors are controlled by the WFGS2 control computer (a Linux machine) which is located just near WFGS2 and can communicate with other computers of UH 88 with Ethernet.

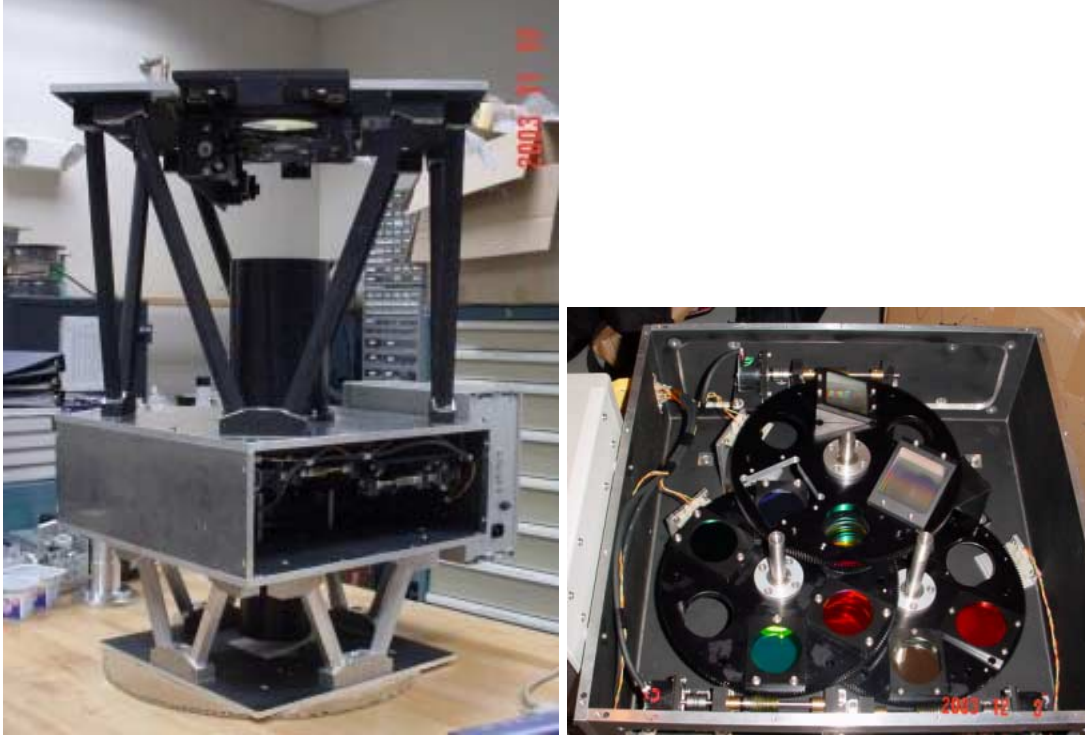


Figure 4. The outside and inside of WFGS2, left: outside view, right: inside view of the wheel box.

4. FIRST LIGHT OBSERVATION

4.1. Pretest in the laboratory

We tested the imaging performance of the optics before the first light observation by using a $35\ \mu\text{m}$ pin hole and confirmed that the full widths at half maximum (FWHM) of spots in the imaging mode are less than 2.2 pixels of Tektronix 2k CCD. These are almost the same as the design values. The light source used in this test had a smaller f-number than that of the UH88 telescope. Therefore, the real FWHM of spots are supposed to be smaller than the measured values.

4.2. Observation

The first light observation was done on the UH88 telescope at Mauna Kea on 2003 November 24 - 30. During this observation, we found some minor mechanical problems which can be fixed by the next observation. We were able to obtain only a small amount of data. We present the results of the first light observation in Figure 5 and 6.

The left of Figure 5 is i' -band slit-less spectroscopic image of the spectrophotometric standard star LTT9239 with a 120 sec exposure. The brightest spectrum near the center of the image corresponds to LTT9239. The right image of Figure 5 is the supernova remnant Crab Nebula. This image is a false color image (g' : blue and green, r' : red). The exposure times are 10 sec at g' and 1 sec at r' . Vignettes are seen at four corners of the Figure 5 images. This is due to the shutter diameter whose size is smaller than that of the convergence beam.

The spectrum of the Eskimo Nebula is shown in Figure 6. This is obtained in the long-slit spectroscopic mode. The $\text{H}\alpha$, $\text{H}\beta$ and $[\text{OIII}]$ lines are clearly seen. The two lines of $[\text{NII}]$ are identified with $R = 630$. The emission lines near $\lambda = 1000\ \text{nm}$ come from the 2nd order diffraction light of $\lambda \sim 500\ \text{nm}$. These emission lines will be removed with a lowpass filter in the near future.



Figure 5. Image of slit-less spectroscopy and imaging, left: i' -band image of the spectrophotometric standard LTT9239 with 120 sec exposure, the brightest spectrum is LTT9239, right: false color image of the Crab Nebula (blue: g' 10 sec exposure, green: g' 10 sec exposure, red: r' 1 sec exposure).

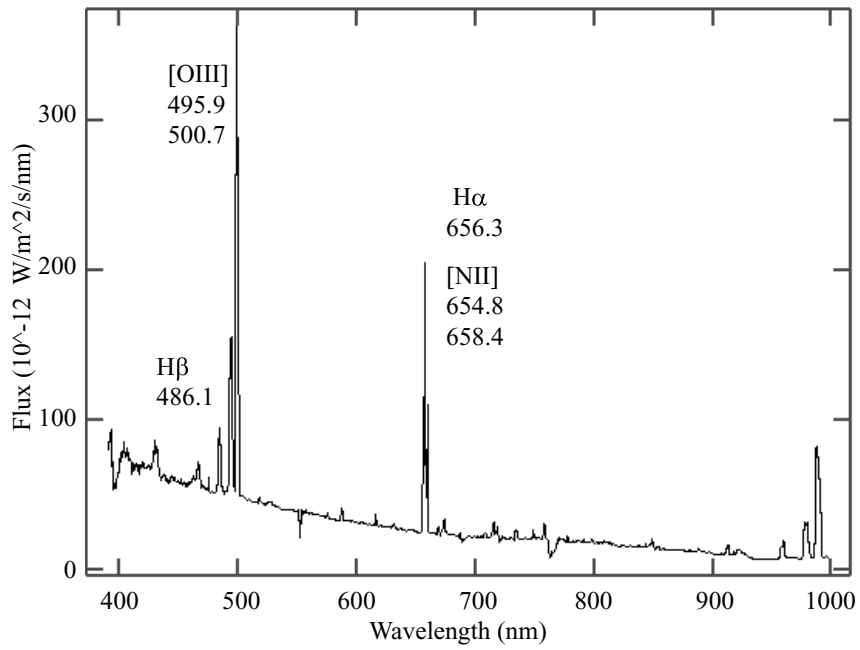


Figure 6. Spectrum of the Eskimo Nebula in the long-slit spectroscopic mode.

4.3. Performance of WFGS2

We evaluated the performance of WFGS2 by analysing a few data (Table 4). The FWHM of point spread function (psf) was measured to be 2.4 pixel under the relatively good seeing conditions although the weather conditions were poor. It seems to be rather good. The measured dispersions of both replica gratings are nearly the same as the design values. In the case of the 300 gr/mm grism, the measured resolutions are also the same as the design values. On the other hand, the resolutions of the 600 gr/mm grism are lower than the design ones because of the defocus at $\lambda \sim 400$ nm. They would become better at the focal point. Thus, we confirmed the good performance of WFGS2 with 300 gr/mm grism. We will further reevaluate the spectroscopic performance with 600 gr/mm and VPH gratings in the next observation.

Table 4. Spectroscopy performance in the first light observation

	Design		Measured	
	300 gr/mm at 650 nm	600 gr/mm at 400 nm	300 gr/mm at 660 nm	600 gr/mm at 400 nm
Dispersion (nm/pixel)	0.38	0.19	0.38 ± 0.1	0.19 ± 0.1
Resolution				
0" .6 slit	960	1100	890	(510)
0" .9 slit	620	730	630	(470)

5. SUMMARY

We developed WFGS2. The wide field of view of $11'.5$ and wide wavelength coverage of 380 - 970 nm are confirmed to be achieved.

The spectroscopic performance with 300 gr/mm grism is good, almost the same as that of the original design. Since the WFGS2 performance tests have not been fully done due to very bad weather during the first light run, we would like to reevaluate it, including the performance of the 600 gr/mm and VPH gratings, in the next observations after improving WFGS2 and installing the VPH grism.

ACKNOWLEDGMENTS

We thank the graduate students of Z-lab, the staff of the machine shop of Department of Physics, Nagoya University for helps and suggestions on the WFGS2 development. We also thank the staffs of the UH 2.2 m telescope and the Subaru Observatory and the National Astronomical Observatory of Japan for supporting the first light run of WFGS2.

WFGS2 is supported by the Daiko Foundation and by the Sumitomo Foundation. This instrument is also supported by Grants-in-Aid from the Ministry of Education, Culture, Sports, Science and Technology (14540228 and 15540238).

REFERENCES

1. Ogura, K., Sugitani, K., Pickles, A., "H α Emission Stars and Herbig-Haro Objects in the Vicinity of Bright-rimmed Clouds", *AJ*, 123, 2597, 2002.
2. Fukugita, M., Ichikawa, T., Gunn, J. E., Doi, M., Shimasaku, K., Schneider, D. P., "The Sloan Digital Sky Survey Photometric System", *AJ*, 111, 1748, 1996.
3. Barden, S. C., Arns, J. A., Colburn, W. S., Williams, J. B., "Volume-Phase Holographic Gratings and Efficiency of Three Simple Volume-Phase Holographic Gratings", *PASP*, 112, 809, 2000
4. Ebizuka, N., Oka, K., Yamada, A., Watanabe, M., Shimizu, K., Kodate, K., Kawabata, M., Teranishi, T., Kawabata, K., Iye, M., "Development of Volume Phase Holographic (VPH) Grism for Visible to Near Infrared Instruments of the 8.2m Subaru Telescope", *SPIE*, 4842, 319, 2003